Authors' Response to Reviews of

WES-2025-69: Modelling vortex generators effects on turbulent boundary layers with integral boundary layer equations

Abhratej Sahoo, Akshay Koodly Ravishankara, Wei Yu, Daniele Ragni, and Carlos Simao Ferreira
Wind Energy Science, doi.org/10.5194/wes-2025-69

RC: ***Reviewer's Comment***, AR: Authors' Response, ☐ Manuscript Text

1. Reviewer 1

RC: ***I think the work has significance for the scientific community. As described by the authors, similar development has been done in the past, but the present work removes some of the assumptions behind those, to get higher accuracy/realism in the simulations. This is well explained in the text, which is also a summary of the VG modelling by meaning of panel code and highlights the next steps to further improve***

AR: We thank the reviewer for their positive comments and time reading the paper.

2. Reviewer 2

RC: ***The paper is nicely written and easy to read. First, a CFD RANS simulation is made over a flat plate with VGs to investigate the boundary layer parameters for zero pressure gradient. Based on this some functions are made that can with some success model the spanwise variation of the shape factor, H, see Figure 6a and an excellent agreement of the spanwise averaged value, Figure 6b. This is only shown at a distance of 10 heights from the VGs and it could be nice to also see if this iis equally valid at some other distances.***

AR: We thank the reviewer for their time and their comments about the readability of the paper. Figures 1a and 1c shows plots comparing the CFD computed and modelled shape factor H at 5 and 15 heights downstream of the VG location. We will also add these plots in the revised manuscript as subplots a and c to Figure 6. As mentioned in lines 215-217 of the original manuscript, we aim to consistently integrate the new VG model with the original 2D Integral Boundary Layer (IBL) framework of RFOIL/XFOIL. Consequently, we make a choice to focus on accuracy in predicting the span-averaged values of the shape factor H.

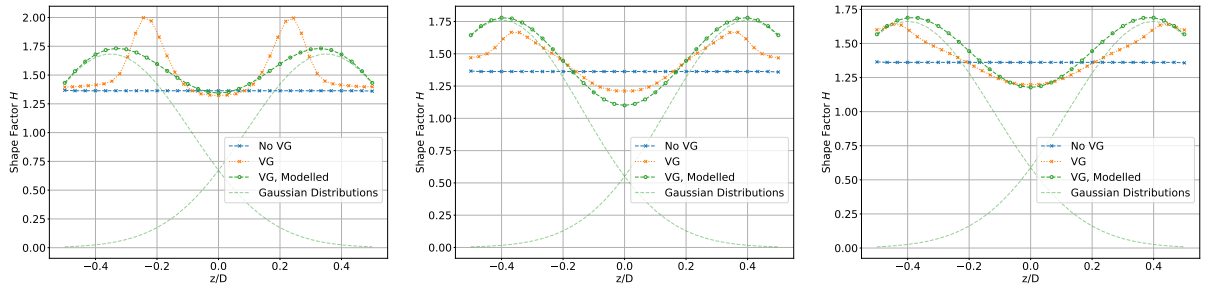

(a) Spanwise distribution at $\frac{x-x_{VG}}{h_{VG}} = 5.0$ (b) Spanwise distribution at $\frac{x-x_{VG}}{h_{VG}} = 10.0$ (c) Spanwise distribution at $\frac{x-x_{VG}}{h_{VG}} = 15.0$

Figure 1: Comparison of actual shape factor from CFD to the model approximation as the sum of two Gaussian distributions at streamwise locations downstream of the VGs for a flat plate with VGs of 5 mm height at 2 million Reynolds number.

RC: ***It is a bit strange to apply a compressible solver even though this is capable with a preconditioner to model an incompressible flow.***

AR: We agree with the reviewers comments about using preconditioners in compressible solvers for incompressible flow. We also make use of such preconditioners in this work and mention them in lines 126-127 of the paper. The SU2 solver has been widely demonstrated as capable of modelling incompressible flows relevant to wind energy applications by both academia and industry (e.g. in [1–3]) and is thus widely used in the authors' research groups. The choice of solver was also a practical one, as SU2 is quite beginner-friendly for solver setup and meshing.

RC: ***There is something wrong with the units in the extra terms in Eqs. 6 and 7, e.g. the extra term including the induced pressure from the VGs has dimension N/m^2 and the other terms are dimensionless in the equation. The last term in Eq 7 is dimensionless, but not the second last.***

AR: We agree with the reviewer and thank them for pointing out the typo of missing non-dimensionalising terms. The equations are presented below in Equations (1) and (2) with the missing non-dimensionalising terms highlighted and will be rectified in the revised manuscript.

$$\frac{d\overline{\theta}}{dx} = \frac{\overline{C_f}}{2} - \left(\overline{H}+2\right)\frac{\overline{\theta}}{U_e}\frac{dU_e}{dx} + \frac{1}{\rho U_e^2}\overline{\left(\int_0^{\infty}\frac{\partial p_{i,VG}}{\partial x}dy\right)} \tag{1}$$

$$\frac{d\overline{H^*}}{dx} = 2\frac{\overline{C_{\mathcal{D}}}}{\overline{\theta}} - \frac{\overline{H^*}}{\overline{\theta}}\frac{\overline{C_f}}{2} + \left(\overline{H}-1\right)\frac{\overline{H^*}}{U_e}\frac{dU_e}{dx} + \frac{2}{U_e^3\overline{\theta}}\overline{\left(\int_0^{\delta}\tau_{zx}\frac{\partial u}{\partial z}dy\right)} + \frac{2}{\rho U_e^3}\overline{\left(\int_0^{\delta}u\frac{\partial p_{i,VG}}{\partial x}dy\right)} \tag{2}$$

RC: ***It is written that pi,VG is the induced pressure from the presence of the VGs, but it is not clear how this is computed. A lot more details on the coupling and the closure terms are needed.***

AR: The derivation of the VG IBL equations and verification of the closure relations were presented in Appendices A and B in the original manuscript. To highlight clearly the derivation process and significant new terms in the equations, these have been moved to the main text in section 4, with some edits made to ensure smooth readability of the text. The text on modelling and implementing the new IBL equations for VGs in RFOIL has been split away from section 4 to a new section 5. The revised manuscript now clearly highlights the exactness of derivation of the new IBL equations in section 4 and the fact that the VG model is only needed to implement the new equations in RFOIL in section 5. The structure of the sections in the revised manuscript is presented below.

4 Modified IBL Equations for VGs
...
4.1 A note on Spanwise Averaging
...
4.2 Deriving the Modified IBL Equations for VGs
...
4.3 Verifying the validity of closure relations for VGs
...
5 Modelling the VG IBL equations in RFOIL
...
5.1 Choosing the most significant VG IBL terms to model
...
5.2 Modelling the Shape Factor
...
5.3 Modelling the Viscous Dissipation Coefficient
...
5.4 Modelling transition to turbulence and upstream effects
...

6 Verification of the new VG model
...
7 Validation of the new VG Model in RFOIL
...
8 Global Performance Assessment
...
9 Conclusions and Future Work
...

RC: ***And an important reference to Ramos-Garcia et al is missing, that also made some improvements to XFOIL and where results are quite good for clean airfoils, "A strong viscous-inviscid interaction model for rotating airfoils, Wind Energy 2014 (17)"***

AR: We agree with the importance of the work of Ramos-Garcia et al for rotating clean airfoils, but do not see the relevance to vortex generator (VG) modelling. As mentioned in lines 98-100 in the original manuscript, we only modify the IBL framework for VGs while retaining RFOIL's pre-exisiting models for rotating and thick airfoils. We are happy to include any missing relevant references to VG modelling in IBL.

RC: ***The first test case of a thin airfoil with a very low angle of attach gives reasonable results for the BL parameters, but the skin friction Cf I Figure 11c is quite off, also without VGs, but that is not contributed to the extra VG terms but the general IBL.***

AR: We agree with the reviewer on the IBL framework's pre-existing shortcomings in modelling the skin friction even without VGs.

RC: ***Then it was chosen to compare results against two old measurements, one made in the Velux tunnel and another using the TUDelft WT. The Velux tunnel data are old and of not so high quality and made at very high inflow turbulence and the TUDelft WT much better. None of the results are very good and overshoots Cl,max, but it is known that computing thick airfoils is difficult and wind tunnel measurements are also not easy since the flow is 3-D. But it is not so convincing that RFOILVG is much better than the older versions.***

AR: The complete list of datasets used to benchmark the models can be found in Appendix C of the original manuscript (appendix A in the revised manuscript). The global performance assessment of the new model for all these datasets is discussed in section 8 of the original manuscript. To highlight a dataset not from the Velux or TU Delft tunnels, we will add a subsection in the revised manuscript (section 7.3) comparing the VG models on an FFA-W3-301 airfoil that was measured in the Stuttgart Laminar Wind Tunnel. The lift performance prediction for the FFA-W3-301 airfoil is presented here in Figure 2. Overall, the new RFOILVogue model produces a smaller error in stall angle and maximum lift predictions compared to the older RFOILVG for a wide range of airfoils, as shown in performance statistics in Table 2 of the original manuscript. The FFA-W3-241 and the DU-97-W-300 airfoils were highlighted in the original manuscript because of the wide variety of VG parameters covered for both free and forced transition in the experimental datasets. The inflow turbulence level of the Velux dataset is acknowledged in lines 284-285 of the original manuscript and is reflected accordingly in the RFOIL calculation settings used during the benchmark. Mainly in RFOIL calculations, the inflow turbulence level is used to set the critical amplification ratio (N_{crit}) from the e^N transition prediction method [4] for the free transition calculations. The authors agree with the reviewer that reduced-order models such as RFOIL/XFOIL can generally over-predict the maximum lift even for clean airfoils without VGs. The proposed VG model in this work only aims to improve over other existing VG models within the framework of RFOIL, and does not aim to tackle the inherent shortcomings of reduced-order methods based on the Integral Boundary Layer framework. We will revise the conclusions section to make this clear to the readers of the paper.

7.3 Comparison for the FFA-W3-301 airfoil
...

RC: ***The authors mention that there still is work to do with respect to include higher pressure gradients and I recommend that the work is not yet ready for publication in WindEnergyScience.***

AR: We would like to clarify that the mentioned future work refers to improvements for better stall prediction. As such, the derivation of the boundary layer equations and the IBL equations for VGs is exact. The derivation of the equations was

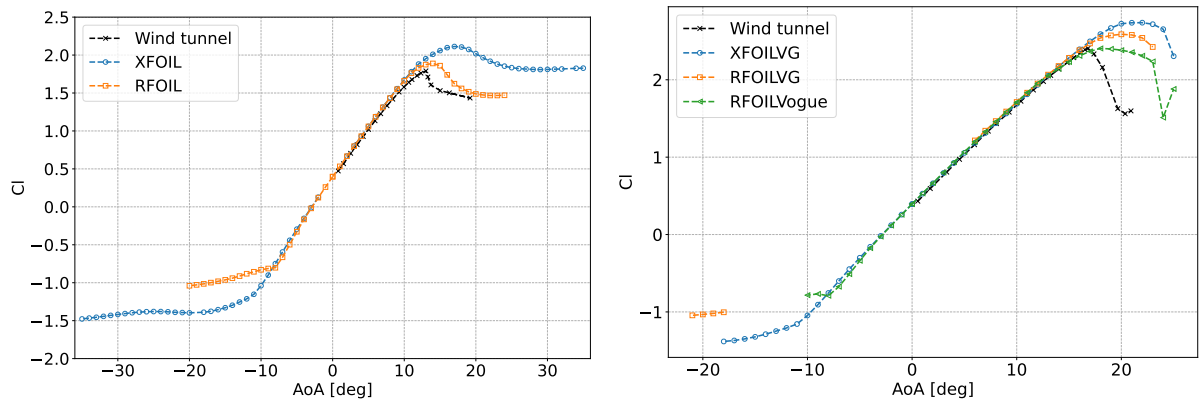

(a) Free transition, no VG

(b) Free transition, VGs at 30% chord

Figure 2: Lift characteristics for the FFA-W3-301 airfoil in free transition with and without VGs placed at 30% chord. Height of the VGs is 1% of the chord length. number. Wind tunnel data taken from [5].

presented in Appendix A and B of the original manuscript and will be moved to the main text as mentioned earlier. To highlight the presence of the adverse pressure gradient contributions, the X-momentum boundary layer equation is presented here in Equation (3), and the IBL equations are presented in Equations (4) and (5). In all these equations, the $\frac{dU_e}{dx}$ terms denote the contribution of the streamwise pressure gradient, which is an adverse pressure gradient in the case of flows on airfoil surfaces. RFOILVogue with the implemented new VG model can predict well flow separation experienced at adverse gradients. To illustrate this, we have included here C_p distributions from the FFA-W3-241 and DU-97-W-300 airfoils at angles of attack with both medium and strong adverse pressure gradients in Figures 3 to 6. Note that the C_p data for the FFA-W3-241 airfoil have been digitised from [6] and thus there may be some minor discrepancies from the source paper. At all angles of attack with adverse pressure gradients where flow separation is expected, RFOILVogue captures flow separation location well. The separation point stays within 5-10% chord lengths of the experiment separation location, as is expected from the no-VG RFOIL calculations. With increasing pressure gradient at high angles of attack, both RFOIL and RFOILVogue tend to predict a larger suction peak, leading to a greater normal force and lift prediction. This is the reason why both RFOIL and RFOILVogue predict well the $C_l - \alpha$ curve before stall, but overpredict the maximum lift. As such, this limitation is also seen in the no-VG RFOIL and not created by the VG model. To make this distinction clearer, and to illustrate the VG model's capabilities at adverse pressure gradients, we will include these C_p distributions in the revised manuscript. We will also revise the conclusions and recommendations section to clearly illustrate the VG model's capabilities with adverse pressure gradients and the inherent limitations of stall prediction in methods like RFOIL.

$$\text{X Momentum Equation:} \quad \overline{u}\frac{\partial \overline{u}}{\partial x} + \overline{v}\frac{\partial \overline{u}}{\partial y} + \overline{w}\frac{\partial \overline{u}}{\partial z} = U_e\frac{dU_e}{dx} - \frac{1}{\rho}\frac{\partial p_{i,VG}}{\partial x} + \frac{1}{\rho}\left(\frac{\partial \tau_{yx}}{\partial y} + \frac{\partial \tau_{zx}}{\partial z}\right) \tag{3}$$

$$\frac{d\overline{\theta}}{dx} = \frac{\overline{C_f}}{2} - \left(\overline{H}+2\right)\frac{\overline{\theta}}{U_e}\frac{dU_e}{dx} + \frac{2}{\rho U_e^2}\overline{\left(\int_0^\infty \frac{\partial p_{i,VG}}{\partial x}dy\right)} \tag{4}$$

$$\frac{d\overline{H^*}}{dx} = 2\frac{\overline{C_\mathcal{D}}}{\overline{\theta}} - \frac{\overline{H^*}}{\overline{\theta}}\frac{\overline{C_f}}{2} + \left(\overline{H}-1\right)\frac{\overline{H^*}}{U_e}\frac{dU_e}{dx} + \frac{2}{U_e^3\overline{\theta}}\overline{\left(\int_0^\delta \tau_{zx}\frac{\partial u}{\partial z}dy\right)} + \frac{2}{\rho U_e^3}\overline{\left(\int_0^\delta u\frac{\partial p_{i,VG}}{\partial x}dy\right)} \tag{5}$$

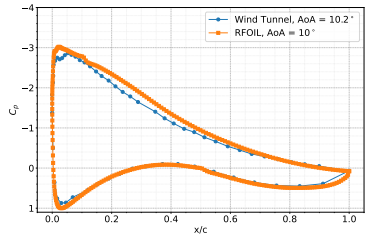

(a) No VG, AoA 10

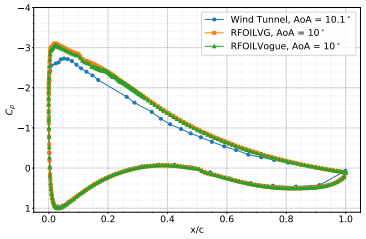

(b) 4mm VGs, $x/c = 0.2$, AoA 10

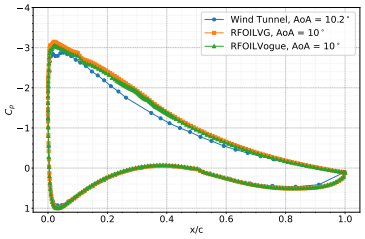

(c) 6mm VGs, $x/c = 0.3$, AoA 10

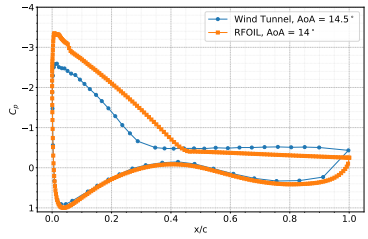

(d) No VG, AoA 14

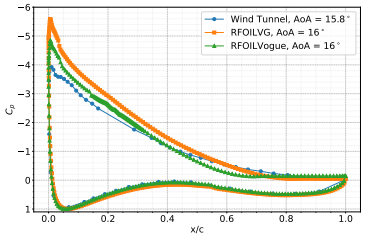

(e) 4mm VGs, $x/c = 0.2$, AoA 16

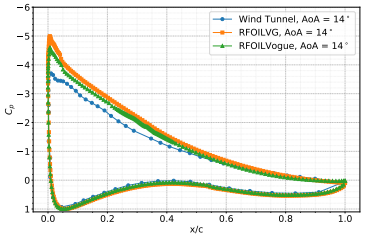

(f) 6mm VGs, $x/c = 0.3$, AoA 14

Figure 3: Chordwise pressure distributions at angles of attack with adverse pressure gradients for the FFA-W3-241 airfoil in free transition at 1.6 million Reynolds number. VGs are placed on the upper surface. Wind tunnel C_p data is digitised from [6].

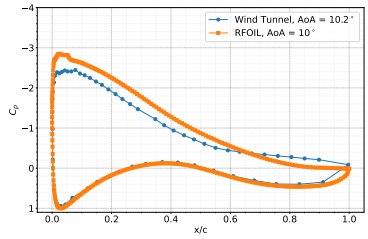

(a) No VG, AoA 10

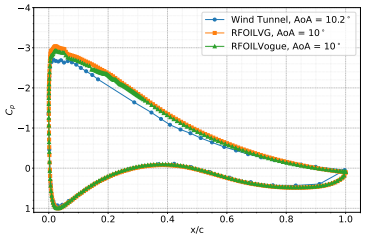

(b) 4mm VGs, $x/c = 0.2$, AoA 10

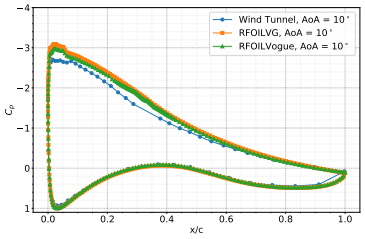

(c) 6mm VGs, $x/c = 0.3$, AoA 10

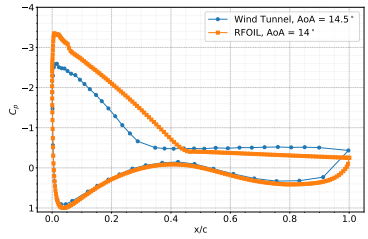

(d) No VG, AoA 14

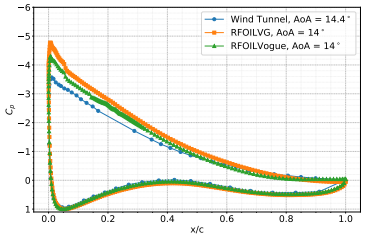

(e) 4mm VGs, $x/c = 0.2$, AoA 14

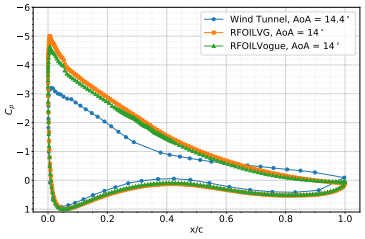

(f) 6mm VGs, $x/c = 0.3$, AoA 14

Figure 4: Chordwise pressure distributions at angles of attack with adverse pressure gradients for the FFA-W3-241 airfoil with forced transition using ZZ tape at 1.6 million Reynolds number. VGs are placed on the upper side. Wind tunnel C_p data is digitised from [6].

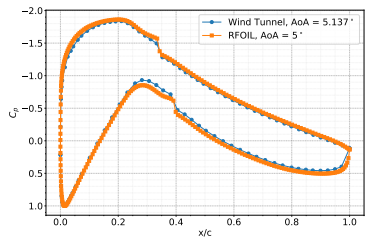

(a) No VG, AoA 5

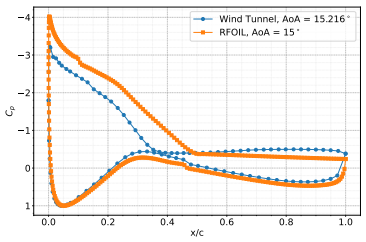

(b) No VG, AoA 15

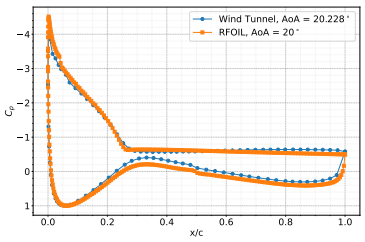

(c) No VG, AoA 20

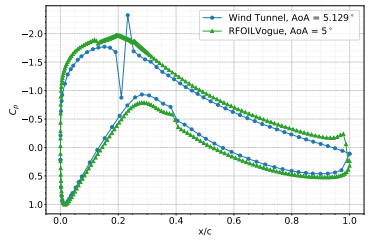

(d) 5mm VGs, $x/c = 0.2$, AoA 5

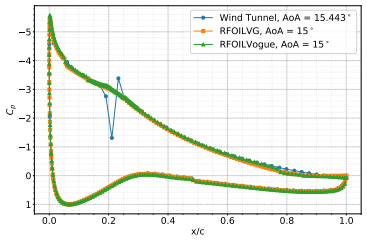

(e) 5mm VGs, $x/c = 0.2$, AoA 15

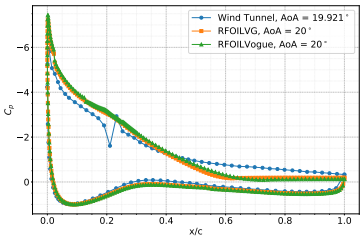

(f) 5mm VGs, $x/c = 0.2$, AoA 20

Figure 5: Chordwise pressure distributions at angles of attack with adverse pressure gradients for the DU-97-W-300 airfoil in free transition at 2 million Reynolds number. VGs are placed on the upper side. The old RFOILVG model does not converge at some angles of attack. Wind tunnel data taken from [7].

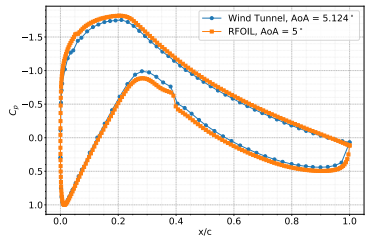

(a) No VG, AoA 5

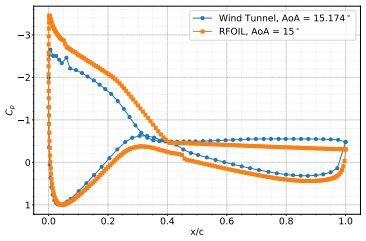

(b) No VG, AoA 15

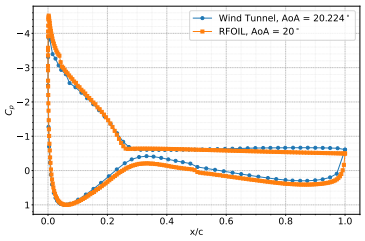

(c) No VG, AoA 20

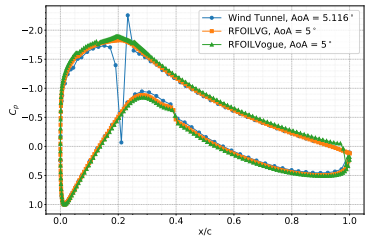

(d) 5mm VGs, $x/c = 0.2$, AoA 5

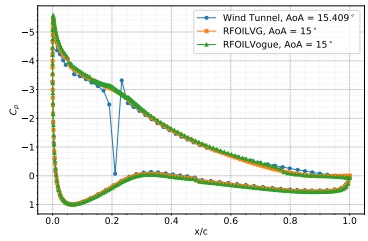

(e) 5mm VGs, $x/c = 0.2$, AoA 15

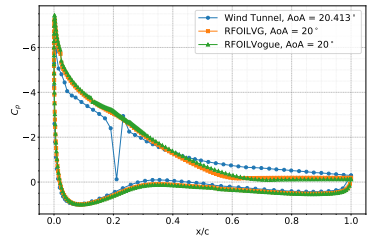

(f) 5mm VGs, $x/c = 0.2$, AoA 20

Figure 6: Chordwise pressure distributions at angles of attack with adverse pressure gradients for the DU-97-W-300 airfoil with forced transition through zigzag tape at 2 million Reynolds number. VGs are placed on the upper side. The old RFOILVG model does not converge at some angles of attack. Wind tunnel data taken from [7].

3. Reviewer 3

RC: ***This paper proposes an integral boundary layer approach to modeling the effect of vortex generators (VGs) for use in reduced-order airfoil aerodynamic analysis tools such as XFOIL / RFOIL. The model is based on flat plate, zero pressure gradient (ZPG) boundary layers. The effect of VGs is modeled through shape factor and viscous dissipation. The model is implemented in RFOIL and is tested for polar predictions for a variety of airfoils. Vortex generator models in XFOIL/RFOIL already exist, however, they model the effect of VGs as an additional source of turbulence in the boundary layer. Such models are highly empirical, employing several tunable coefficients that require training and work well for cases that are used for training, but not as well as for unseen cases. The key contribution of the paper is that the new model is analytical (does not require tuning) and it accounts for changes in flow/momentum in the boundary layer and not just model the VGs as a turbulence source.***

AR: We thank the reviewer for their time reading the paper and highlighting the key contributions of this work compared to previous research on VG modelling.

RC: ***The idea pursued in the paper is good but I see a fundamental issue – at high Reynolds numbers (relevant for wind turbines), stall is caused by turbulent boundary layer separation that progresses (with increasing α) from the airfoil trailing edge to the leading edge. Boundary layer separation is determined almost exclusively by the adverse pressure gradient in such cases and hence models built on a ZPG flow assumption have inherent limitations. This can be seen in the results presented in the manuscript. A systematic study can be performed with the numerical setup discussed in Section 3 to investigate the effect of adverse pressure gradients. The upper boundary in the simulation can be modeled as a wall and its geometry modified to prescribe a pressure gradient distribution on the bottom flat plate with VGS. CFD simulations can be performed for varying magnitudes of adverse pressure gradient (APG) and the proposed model can be a) tested against the data, and b) potentially improved using the data. Given the critical importance of APG, I feel its inclusion is critical. Even if it is not included, a comparison against CFD for a systematically performed analysis of the effect of APG would add tremendous value.***

AR: We disagree with the reviewer about the new VG model's poor performance at high angles of attack with strong adverse pressure gradients and flow separation over the airfoil. To illustrate this, we presented the Cp distributions for free and forced transition with and without VGs for the FFA-W3-241 and DU-97-W-300 airfoils at angles of attack with strong adverse pressure gradients and turbulent boundary layer separation over the airfoil surface in our response to a similar comment by Reviewer 2, and thus refer the reviewer to Figures 3 to 6 in this addendum for these pressure distribution plots. Since the FFA-W3-241 airfoil data had to be digitised from [6], there may be some digitisation errors compared to the source material. Nevertheless, for both airfoils under a wide range of conditions, the new VG model predicts well the extent of separated flow over the airfoil. The separation point stays within 5-10% chord lengths downstream of the experiment separation location, as is expected from the no-VG RFOIL calculation trends. As also mentioned in our response to Reviewer 2's comments, the derivation of the boundary layer equations and IBL equations for VGs is exact without assuming a Zero Pressure Gradient. The $\frac{dU_e}{dx}$ terms in the boundary layer equation (Equation (3)) and IBL equations (Equations (4) and (5)) denote the contribution of the pressure gradient in the governing equations. The derived IBL equations are exact, and the new VG model is only required to implement these equations in RFOIL. Furthermore, the VG model parameters are scaled with Re_θ, thus making the model capable of handling a wide range of boundary layers. We will include both the C_p distribution plots in the revised manuscript to clearly illustrate the capabilities of the new VG model under flow separation due to adverse pressure gradients.

While we agree with the reviewer that a systematic analysis of the VG model's capabilities for controlled adverse pressure gradients and flow separation locations with respect to the VG location will add value, this is currently outside the scope of the project. Nevertheless, we believe that the inclusion of the C_p distribution plots at various high angles of attack and highly adverse pressure gradients in the revised manuscript will clearly indicate the capabilities of the new VG model to the readers.

RC: ***Comparing Figs. 12 and 13 in the manuscript shows a significantly increased discrepancy between the $C_l - \alpha$ curves with the VG models (not only the proposed model, but also the existing RFOILVG model). This increased discrepancy is seen in every case. What causes this? Surface C_p distributions can be plotted to compare if the loss of lift is occurring due to a higher trailing edge flow separation, or something else.***

AR: We have shown Cp distributions for free and forced transition with and without VGs for the FFA-W3241 airfoil in Figures 3 and 4 in this addendum. The wind tunnel C_p data is available for limited angles of attack and digitised from

[6]. Thus, there may be some minor discrepancies with the source paper. All of RFOIL, RFOILVG, and RFOILVogue predict a larger suction peak for this airfoil compared to wind tunnel measurements. The suction peak overprediction increases with increasing angle of attack. In addition, all RFOIL versions predict separation further downstream than the respective wind tunnel measurements. These reasons lead to a particularly higher lift prediction than wind tunnel measurements for this airfoil both with and without VGs. RFOIL predicts a comparatively lower overprediction in the suction peak for other airfoils (e.g. the DU-97-W-300 airfoil, as shown in Figures 5 and 6) for a comparatively lower overprediction in lift. We will include these pressure distributions and their explanation in the revised manuscript.

RC: ***The authors claim in some places that the stall position and post-stall characteristics are predicted better with the proposed model. Looking at it from a physical perspective, the VGs should be ineffective (or at least its modeling would be highly inaccurate) post moment stall as the flow over the airfoil is fully separated. What is the rationale that the "improved" model is because of accuracy.***

AR: We feel there is a mixup in terminology and we acknowledge the inconsistent use of terminology from our side in some parts of the original manuscript. Our intention was to elaborate on the ability of the VG model to better predict the stall angle of attack and the flow separation location when flow separation only spans a part of the airfoil surface. Indeed, when flow separations spans the full airfoil surface, the VGs are ineffective. We will revise the text for the use of correct consistent terminology such that readers can clearly distinguish between flow separation and stall in the explanations provided in the text. Additionally, the pressure distributions over the discussed airfoils at various angles of attack will also make the text in the revised manuscript much clearer.

RC: ***A passing remark is made about improved robustness of the proposed model in the conclusion. This should be elaborated on and put in the main paper.***

AR: We will split section 8 on the global performance assessment (section 7 in the original manuscript) into section 8.1 on accuracy, and section 8.2 on robustness. Briefly, the robustness improvement is seen mainly in free transition cases. The new RFOILVogue converges for more angles of attack in free transition cases compared to the old RFOILVG, especially for lower angles of attack. This is mainly attributed to the more accurate setting of the forced transition location upstream of the VG location for the VG cases, as described in section 4.4 of the original manuscript. This causes the RFOIL code to first switch to the turbulent IBL formulation from the laminar IBL formulation upstream of the VG location, and then switch to the VG formulation at the VG location. Numerically, this leads to smoother gradients, ensuring a converged solution when calculating the IBL quantities in RFOILVogue, as opposed to a sharp change at the VG location, causing RFOILVG to not converge. The effect of a more accurate forced transition location is only observed at low angles of attack when the natural transition location is downstream or close to the VG location. At higher angles of attack, natural transition occurs far upstream of the VG location, and thus, transition location fixing is never activated. Consequently, calculations from both VG models converge as usual. As an illustration, Figure 7 highlights some cases where RFOILVogue converges for more angles of attack than RFOILVG in free transition. We will also add this figure to the revised manuscript.

8 Global Performance Assessment
...
8.1 Accuracy
...
8.2 Robustness
...

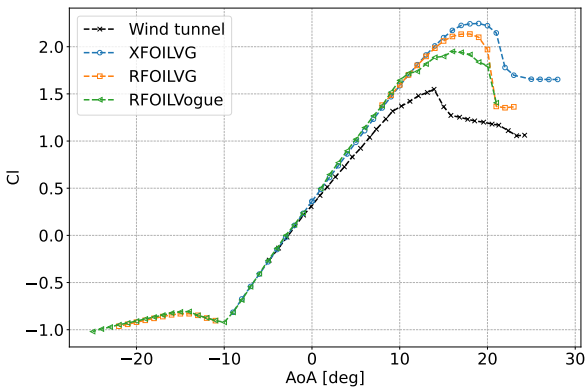

(a) FFA-W3-241, free transition, VGs of height 6 mm placed at $x/c = 0.3$.

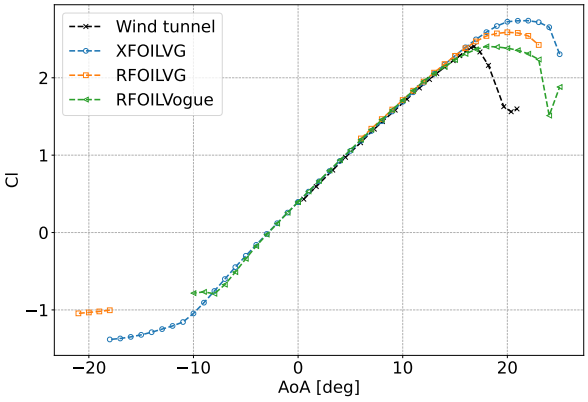

(b) FFA-W3-301, free transition, VGs of height $h_{VG}/c = 0.01$ placed at $x/c = 0.3$.

Figure 7: Lift characteristics for the FFA-W3-241 and FFA-W3-301 airfoils in free transition with VGs. RFOILVG calculations only converge AoA 8 onwards for the FFA-W3-241 airfoil, and AoA 6 onwards for the FFA-W3-301 airfoil, instead of the full range. Wind tunnel data taken from [5, 6].

References

1. Ravishankara, A. K., Bakhmet, I. & Özdemir, H. Estimation of roughness effects on wind turbine blades with vortex generators. *Journal of Physics: Conference Series* **1618,** 52031 (2020).
2. Vimalakanthan, K., Caboni, M., Schepers, J., Pechenik, E. & Williams, P. Aerodynamic analysis of Ampyx's airborne wind energy system. *Journal of Physics: Conference Series* **1037,** 062008. ISSN: 1742-6588 (June 2018).
3. Barrett, R. & Ning, A. Comparison of airfoil precomputational analysis methods for optimization of wind turbine blades. *IEEE Transactions on Sustainable Energy* **7,** 1081–1088 (July 2016).
4. Van Ingen, J. L. The eN method for transition prediction. Historical review of work at TU Delft. *38th AIAA Fluid Dynamics Conference and Exhibit* (2008).
5. Sorensen, N. N., Zahle, F., Bak, C. & Vronsky, T. Prediction of the Effect of Vortex Generators on Airfoil Performance. *Journal of Physics: Conference Series* **524,** 012019. ISSN: 1742-6596 (June 2014).
6. Fuglsang, P. L., Antoniou, I., Dahl, K. & Madsen, H. A. Wind tunnel tests of the FFA-W3-241, FFA-W3-301 and NACA 63-430 airfoils. *Riso-Reports-Riso R* **1041,** 1–163. ISSN: 0106-2840 (1998).
7. Baldacchino, D., Ferreira, C., Tavernier, D. D., Timmer, W. & van Bussel, G. J. W. Experimental parameter study for passive vortex generators on a 30% thick airfoil. *Wind Energy* **21,** 745–765. ISSN: 1095-4244 (Sept. 2018).